Clim Dyn (2015) 45:1–20
DOI 10.1007/s00382-015-2532-2

Energetics of wave propagation leading to cold event in tropical latitudes of South America

Gabriela Viviana Müller · Manoel Alonso Gan · Everson Dal Piva · Virginia Piccinini Silveira

Received: 22 February 2014 / Accepted: 13 February 2015 / Published online: 3 March 2015

Abstract This paper presents a new vision on the cold and cool events that affect the tropical region of South America, considering the dynamics and the energetics of wave train propagation associated with these systems. Through a composite analysis of meridional winds at 300 hPa for cold ($T < 0$ °C) and cool (0 °C $\leq T \leq 2.5$ °C) air incursions affecting tropical latitudes and causing frost are studied. The cold events observed in tropical latitudes are associated with a single Rossby wave pattern propagating over the Pacific Ocean which drives the low level anticyclone from the southwest of the continent to low latitudes. This propagation involves a southern circulation due to the meridional wind penetration and consequently cold air advection causing temperatures to drop below 0 °C. During cool events a subtropical wave train propagating through the Pacific Ocean is observed, which merges before the event with a wave coming from the subpolar latitudes of the South Atlantic Ocean. The zonal propagation leads to the entrance of the anticyclone from the west of the continent, and it is strengthened together with the meridionaly extended cyclone located upstream. This configuration causes southerly wind advection over central-southeastern Brazil and consequently causes the temperature decrease. The energetics shows that the cold events kinetic energy maxima are more intense than those of cool events. For the cold events three maxima are observed, the first (K1) and the third (K3) maxima are developed by baroclinic conversion and ageostrophic flux convergence and the second one (K2) by ageostrophic flux convergence. For the cool events two maxima are found, the first maximum (K4) developed by baroclinic conversion and the second one by ageostrophic flux convergence.

Keywords Energetics · Wave propagation · Frost events · South America

1 Introduction

Cold surges from mid-latitudes in some occasions can produce an important drop in temperature and consequent frost in tropical latitudes as studied by Schutz et al. (1998) in Central America and by Fortune and Kousky (1983) in South America. These events have a substantial impact in the agricultural lands of subtropical and tropical latitudes. Two notable examples in Brazil were the frosts which occurred in the São Paulo state of Brazil during May 1979 and July 1981, both studied by Fortune and Kousky (1983). In this study, a long-wave pattern amplifying over the South Pacific three or 5 days before the freeze event occurred was observed as being a precursor. Marengo et al. (2002) show that the large amplitude upper-level trough in middle latitudes, which extends into the tropics, is one of the major features of the cold situation. These waves embedded in westerly flow are an example of wintertime tropical–extratropical interactions leading to cooling in southeastern South America. Pezza and Ambrizzi (2005)

G. V. Müller (✉)
Centro de Investigaciones Científicas y Transferencia de Tecnología a la Producción (CICYTTP/CONICET), Materi y España, s/n, CP 3105 Diamante, Entre Ríos, Argentina
e-mail: gabrielamuller@cicyttp.org.ar

M. A. Gan · V. P. Silveira
Centro de Previsão de Tempo e Estudo Climáticos, Instituto Nacional de Pesquisas Espaciais (CPTEC/INPE), São José dos Campos, SP, Brazil

E. D. Piva
Departamento de Física, Centro de Ciências Naturais e Exatas, Universidade Federal de Santa Maria, Santa Maria, RS, Brazil

also suggest that the well-defined large-scale wave patterns that can be monitored over the Pacific Ocean up to several days in advance, suggesting a polar connection linking the southeast of Australia with southwestern South America during the preliminary stage. In this sense, Müller et al. (2008) and Müller (2010) demonstrate that wave trains excited by anomalous convections situated in specific oceanic regions and in adequate basic states may propagate across the Pacific Ocean and reach South America with the appropriate phase, creating the local favorable condition which thereby cools the continent.

Marengo et al. (1997) while studying a cool surge occurred in 26 June 1994 in southeastern Brazil, proposed that this event could be associated with an intense positive feedback mechanism between an upper and lower troposphere flow near the Andes prior to the coldest day. An intense trough is produced in the lee side of the Andes due to the low-level cold advection associated with southerlies along the eastern flank of the mountains. On the other hand this trough contributes to generate cold advection along the eastern flank of the Andes, which produces substantial temperature drops and deepens the upper level trough. This intensification produces an increase in the cyclonic vorticity advection, which would tend to produce sea level pressure drops underneath. This near-surface low pressure area would eventually contribute to the southeastern Brazil cooling due to the associated southerly winds.

Based on the synoptic climatology of surface cyclone and anticyclone tracks associated with frosts in São Paulo, Brazil, Pezza and Ambrizzi (2005) showed that there is a preferential trajectory for these systems during frost events. The authors point out that during the previous days to the frost event there were southerly wind anomalies over the southern tip of South America formed due to the geostrophic balance between the developing migratory anticyclone near the southern Chilean coast and the extratropical cyclone over the Atlantic. With the increase of the surface pressure over the southern part of the continent due to the wind anomalies, more air mass is accumulated at the northwest of the high-pressure cell associated with the Andes blocking effect. As a result, the wind velocity and the Coriolis effect are reduced, and a southerly ageostrophic wind component and cold air advection towards lower latitudes at the lee side of the Andes are generated, with the consequent displacement of the anticyclone centre to the north towards the region of maximum cold advection (Gan and Rao 1994; Seluchi et al. 1998; Garreaud 2000).

Among the several precursor conditions for freezing, one of the most important is the amplification of the upper lever wave with a ridge over the west coast and a trough over South America. Fortune and Kousky (1983) observed in Hovmöller ridge–trough diagrams that group-velocity propagation of wave energy from the mid-Pacific contributed to part of the unusual amplification of the cold trough in South America. Similar results were found by Krishnamurti et al. (1999) in their study on the major freeze events throughout southeastern Brazil. They observed downstream amplification of the wave train prior to the freeze event. During the period of frost they found synoptic-scale features centered on zonal wave number 9 receiving energy from lower wave numbers (such as zonal wave numbers via barotropic triad interactions). After the period of the freeze, the baroclinic conversion dominated.

The aim of our study is to identify the difference between the wave train behavior during cool and cold events throughout the tropical region of South America and to verify if the downstream amplification observed by Krishamurti et al. (1999) is associated with agestrophic flux convergence. To attain this goal we explore the energetics of the wave propagation associated with cold and cool surges in the tropical latitude of South America. This study intends to help forecasters to predict cold events following the evolution of propagation wave patterns in the Southern Hemisphere.

2 Event selection criteria, data and methodology

São Paulo meteorological station (23.7°S, 46.6°W), located in a green area in the southern part of São Paulo City, is used as representative of tropical latitudes. Following the classification by Pezza and Ambrizzi (2005, hereafter PA05) from May to September of 1950–2000, the frost events are identified according to the minimum temperature as cold events ($T < 0$ °C) and cool events (0 °C $\leq T \leq 2.5$ °C). For each frost event type (Table 1), composites of meridional wind anomaly in 300 hPa are analyzed in order to study the wave train propagation during the days before the event, as well as composites of 500 hPa geopotential and the terms of Eq. 1 in order to study the energetics, employing the 6-hourly gridded data from NCEP/NCAR reanalysis (Kalnay et al. 1996). The daily anomalies are calculated with

Table 1 Cold and cool surges in São Paulo city from 1950 to 2000 (adapted from Pezza and Ambrizzi 2005)

Cold frost events	Cool frost events
1953/07/05 1955/08/02 1975/07/18	1951/07/06 1953/07/11 1962/07/07
1979/06/01 1990/07/29 2000/07/17	1963/08/06 1964/09/04 1965/07/12
	1968/05/17 1969/07/11 1972/07/09
	1975/07/07 1979/07/18 1981/06/20
	1988/06/06 1993/08/12 1994/06/27

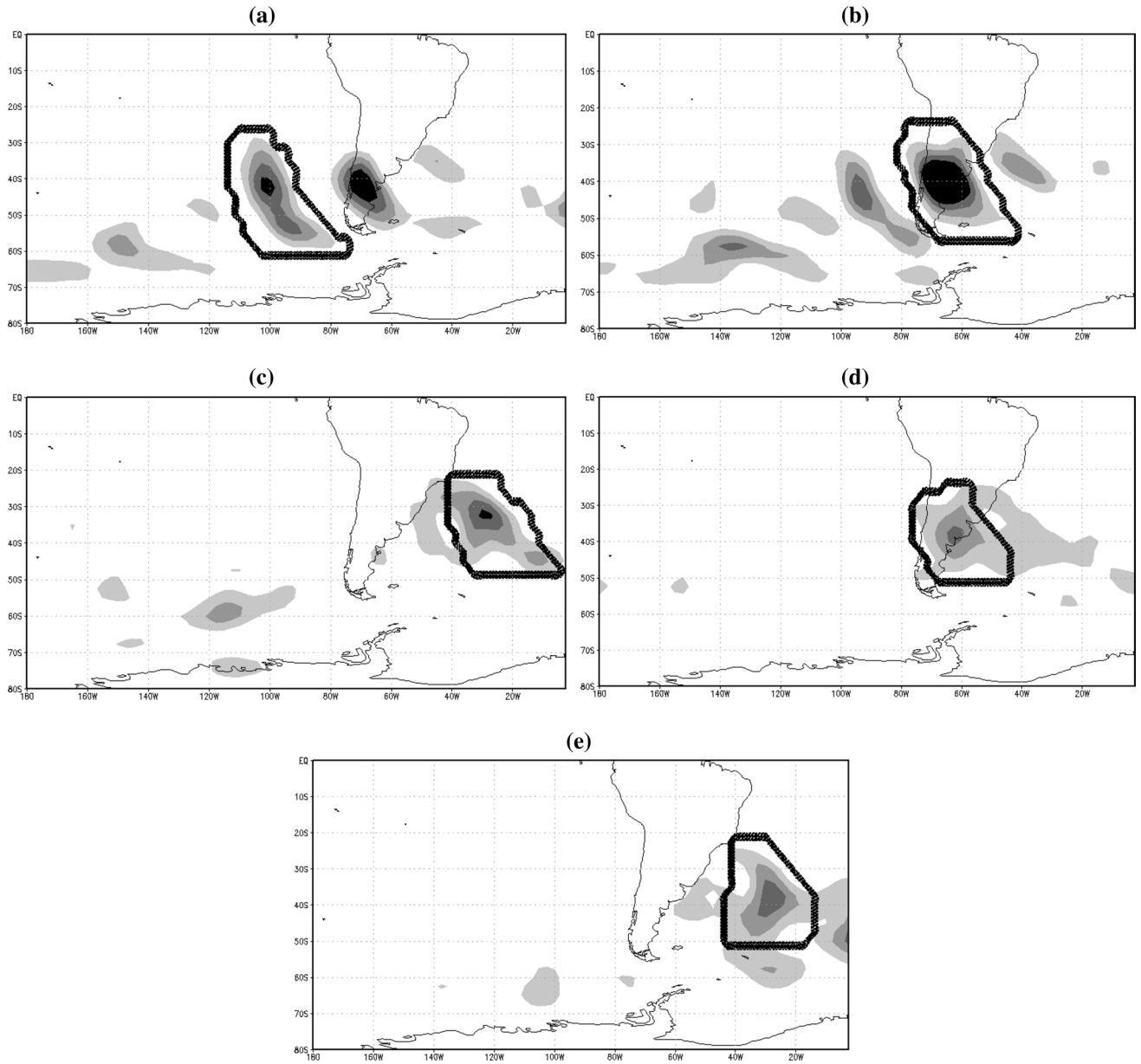

Fig. 1 Vertically averaged eddy kinetic energy ($m^2\ s^{-2}$—*shaded*) and the *cube* (*continue line*) for **a** K1 on Day −3, **b** K2 on Day −2, **c** K3 on Day −0.5, **d** K4 on Day −2 and **e** K5 Day −0.5

respect to the mean value of the period May to September 1950–2000, and the results are tested for statistical significance with the Student's *t* test.

The energetics of the frost event composites is studied through the eddy kinetic energy (K′) equation (Eq. 1) developed by Orlanski and Katzfey (1991) and modified by Chang (2000):

$$\frac{\partial K'}{\partial t} = -\nabla.\overrightarrow{V}K' - \nabla.\overrightarrow{V'_a}\phi' - \omega'\alpha' - \overrightarrow{V'}.\left(\overrightarrow{V'_3}.\nabla_3\right)\overrightarrow{V} + \overrightarrow{V'}.\overline{\left(\overrightarrow{V'_3}.\nabla_3\right)\overrightarrow{V'}} - \frac{\partial}{\partial p}\omega K' - \frac{\partial}{\partial p}\omega'\phi' + RES \quad (1)$$

where $\vec{V}$ is the horizontal wind, the α the specific density, ϕ the geopotential height and ω the vertical wind component in pressure coordinates. In this equation, the overbar denotes a 91-day time mean centered on the Day 0, and the prime the deviation from the average. The subscript "3" in vectors and operators indicates 3-dimensional, while the subscript "a" represents the ageostrophic wind component.

In Eq. 1 the term on the left hand is the local change of K′ with time. On the right hand the first term represents the K′ flux convergence (KFC), the second term represents the ageostrophic flow convergence (AFC), known as the Downstream Development (DSD) term, and the

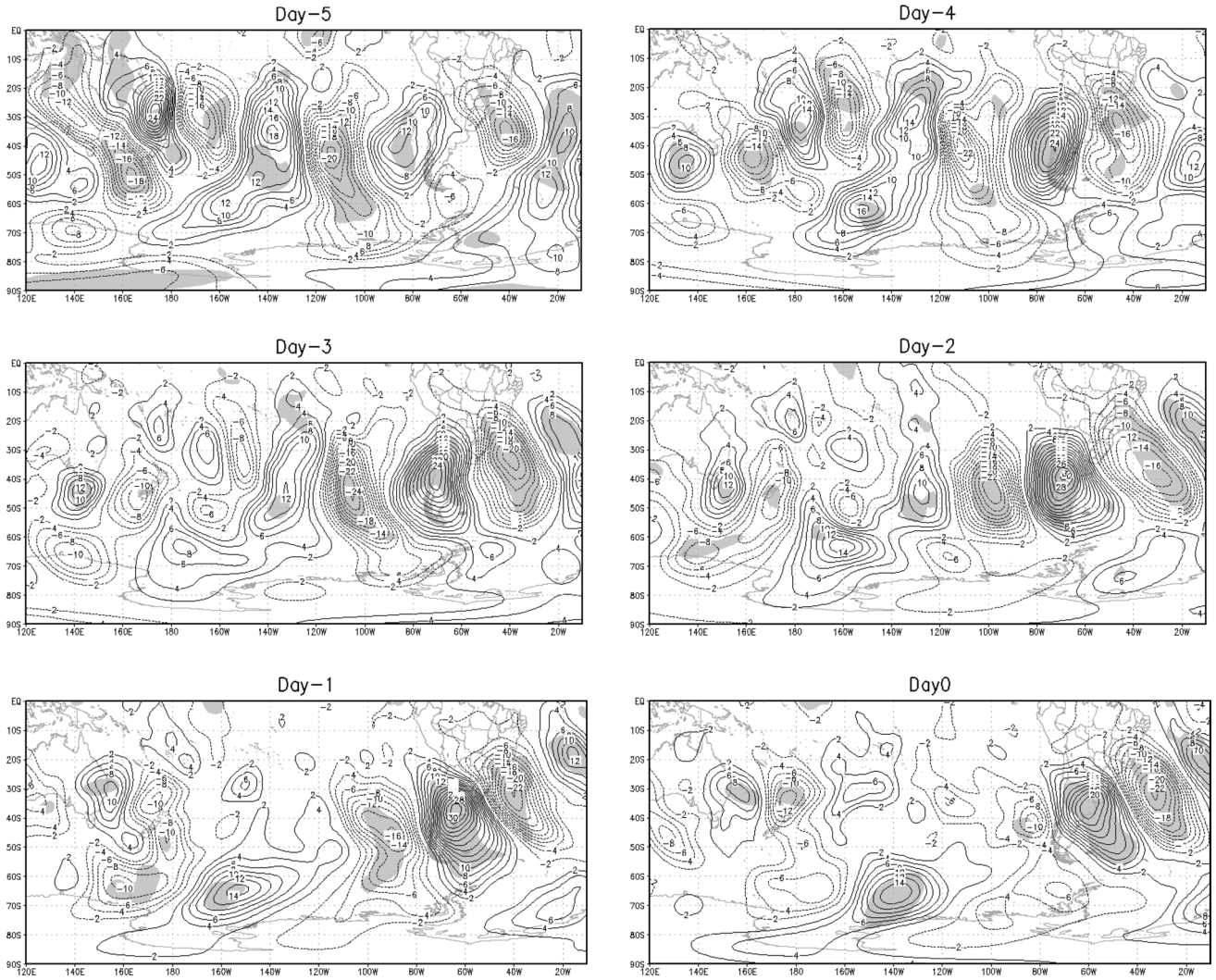

Fig. 2 Meridional wind composites anomaly (ms^{-1}) from Day −5 to Day 0 at 300 hPa, corresponding to cold events. Positive (negative) contours are shown in *solid* (*dashed*) *lines* every 2 m s^{-1}. The *shaded* areas indicate regions with 95 % statistical significance according to a Student's test

third term is the baroclinic conversion (BRC). The fourth and fifth terms represent the barotropic conversion (BRT) because they are associated with the horizontal wind shear. The sixth and seventh terms are associated with the vertical flow convergence of energy. The term RES contains mechanisms not explained by the Eq. 1, such as diabetic heating, friction and mountain effects and other things such as errors introduced by numerical methods. The advantage of studying the energetics using Eq. 1 is that it contains the most important processes for the formation, maintenance and dissipation of the disturbances, such as baroclinic instability, barotropic instability and DSD.

Averaging Eq. 1 over a volume results in the following equation (Chang 2000):

$$\begin{aligned}\frac{\partial\langle K'\rangle}{\partial t} = &-\left\langle\nabla.\vec{V}K'\right\rangle - \left\langle\nabla.\vec{V}'_a\phi'\right\rangle - \langle\omega'\alpha'\rangle \\ &-\left\langle\vec{V'}.\left(\vec{V}'_3.\nabla_3\right)\overline{\vec{V}} + \vec{V'}.\overline{\left(\vec{V}'_3.\nabla_3\right)\vec{V'}}\right\rangle \\ &-\left[\omega K'\right]\big|_B + \left[\omega K'\right]\big|_T - \left[\omega'\phi'\right]\big|_B \\ &+\left[\omega'\phi'\right]\big|_T + \langle RES\rangle \\ &+\left\langle\nabla.\vec{V}_v K'\right\rangle + \left[\left(\frac{\partial p_s}{\partial t} + \vec{V}_v.\nabla p_s\right)K'\right]\Bigg|_B \end{aligned} \quad (2)$$

where the symbol $\langle\rangle$ indicates the volume integral and [] the surface integrals evaluated either at the top (subscript T, taken to be the 100 hPa here), or at the bottom (subscript B taken to be the surface pressure) of the volume; and the subscript "v" represents the volume

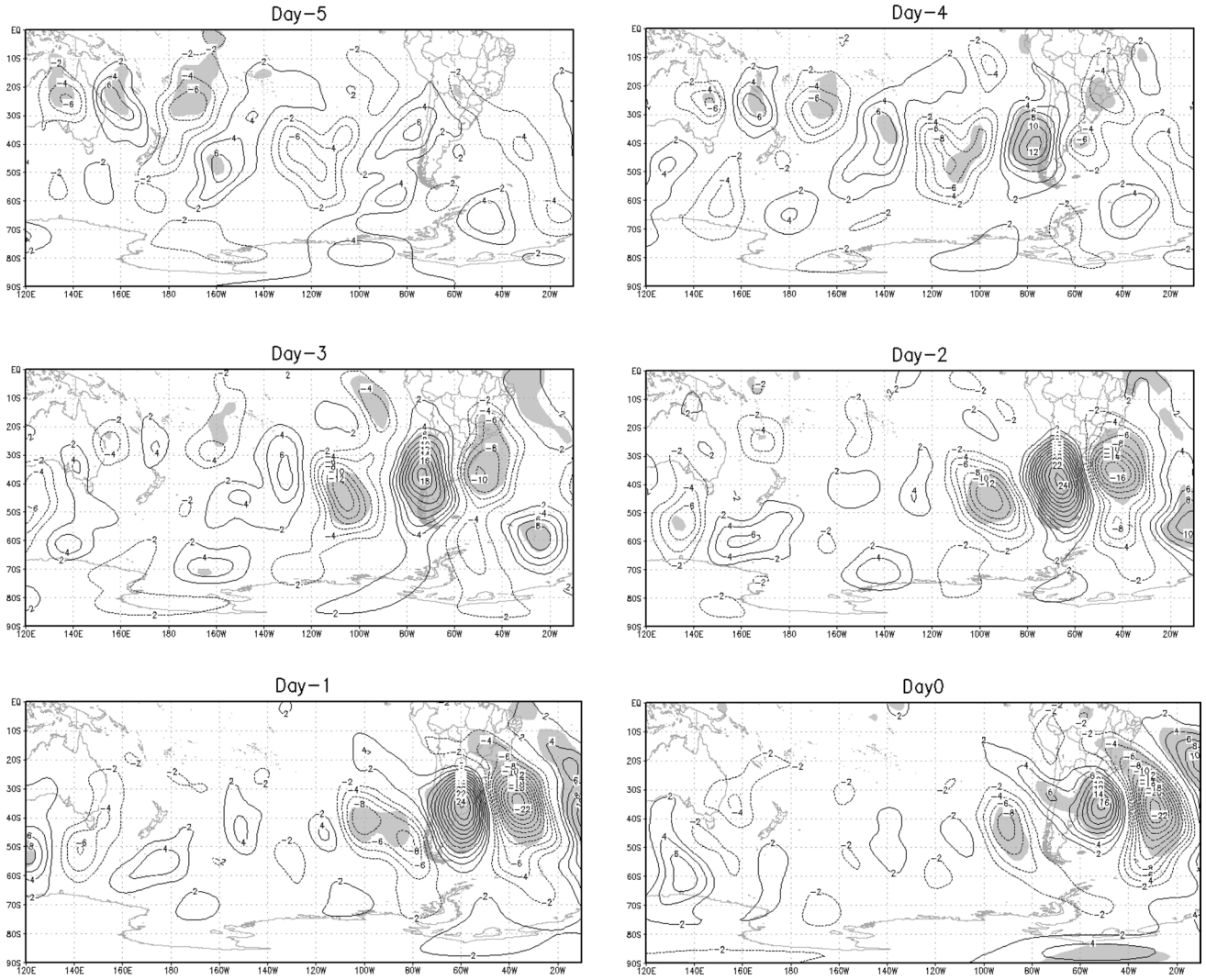

Fig. 3 Meridional wind composites anomaly (m s^{-1}) from Day −5 to Day 0 at 300 hPa, corresponding to cool events. Positive (negative) contours are shown in *solid* (*dashed*) *lines* every 2 m s^{-1}. The *shaded* areas indicate regions with 95 % statistical significance according to a Student's test

displacement velocity. The terms of Eq. 2 have the same interpretation that in Eq. 1, except the two terms representing the vertical flux convergence of energy. The sixth to ninth terms are interpreted as the vertical flux of energy through the lower boundary (B) to the top (T) of the atmosphere. The tenth term represents the energy flux due to the movement of the volume integration, while the last term is the change in the energy due to the variation of the mass in the volume. The time change term was computed in two ways: in the first one a centered time difference was applied between the previous 6 h and the subsequent 6 h (OKT). In the second one, all terms in Eq. 2 were summed, except for the RES term (CKT). The RES term was determined as the difference between these two tendencies. To apply this equation, a cube was defined around each kinetic energy maximum (see black box in Fig. 1). The cube was displaced step by step to follow the maximum propagation of kinetic energy. Vertical levels used for the vertical integration were from the first isobaric level located above the ground used in the reanalysis to the 100 hPa level.

3 Diagnosis of wave train propagation

3.1 Cold frost events

The composites of the São Paulo cold frosts presented in Table 1 are depicted in Fig. 2 which shows the 300 hPa meridional wind field anomalies from Day −5 to Day 0 when the cold event occurs. From this figure it can be seen a well-defined single wave propagation pattern along the

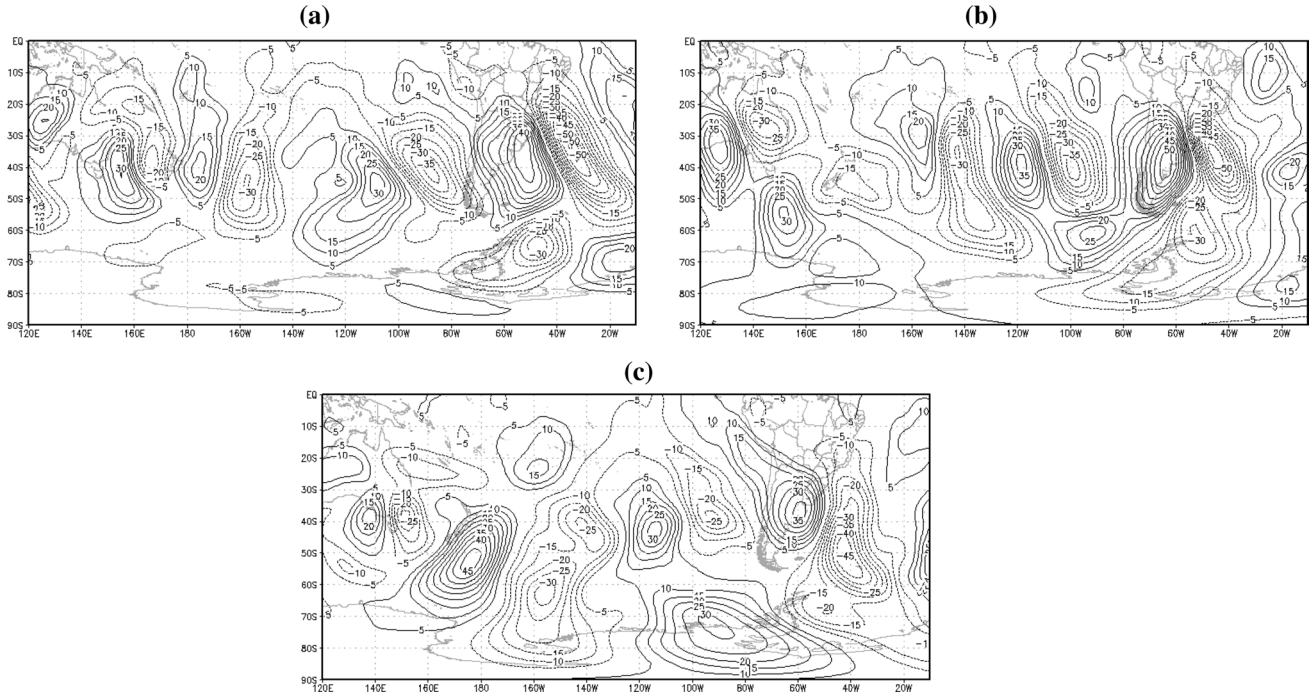

Fig. 4 Meridional wind anomalies (m s^{-1}) at 300 hPa for the Day previous to a cold event **a** 31/05/79 and the cool event **b** 26/06/94 and **c** 6/7/75. Positive (negative) contours are shown in *solid* (*dashed*) *lines* every 2 m s^{-1}

Pacific Ocean with statistically significant (95 %) anomaly values. The anomalies become more intense during the days preceding the event at least from 120°E to the east. This configuration is similar to the cases of less persistent generalized frost events in the Wet Pampas in central-southern South America obtained by Müller and Berri (2007) and resembles typical Rossby wave train propagation pattern for cold air irruptions widely studied in the literature (Fortune and Kousky 1983; Marengo et al. 1997; Garreaud 2000; Marengo et al. 2002; among others). After Day −3 the statistically significant anomalies over the South American region have a slow northeastward displacement. At low-levels, the atmospheric pattern is characterized by a cold front following a southwest-northeast trajectory with post frontal anticyclone entering the continent at high latitudes (figure not shown). From a synoptic classification of sequence patterns of sea level pressure and 500 hPa geopotential heights associated with cold waves over São Paulo City, Escobar (2007) found that this is the first pattern of rotated principal component analysis which explains 29.3 % of the variance. In mid levels, the circulation associated to this pattern consists of an intense ridge in the Pacific Ocean, close to the Chilean coast, and a trough extending from the inner part of the continent to the South Atlantic Ocean, as shown by PA05 and Escobar (2007), among others. The orientation of the upper-level flow between the ridge and the trough is almost from south to north, that contributes to incursions of migratory systems in low levels from southern South America to central-western and southeastern Brazil, as the evolution of a cold wave over South America (i.e., Garreaud 2000; Marengo et al. 1997).

3.2 Cool frost events

Figure 3 depicts the same anomaly field as Fig. 2, but for the cool events (Table 1). A propagation pattern along the subtropical Pacific Ocean is observed in days prior to the event, but with smaller anomaly values during the pre-frost days than cold events, which is coherent with the fact that cool events are less intense than cold events. Another short wave pattern, although not statisticaly significant, is observed in sub-polar latitudes on the previous day, which contributes to the cool events, as shown by Fortune and Kousky (1983) and Vera and Vigliarolo (2000) for freezing episodes over southern Brazil.

From Day −5 to Day −3 a positive 300 hPa meridional wind anomaly is observed to the west of the continent (Fig. 3) being less intense and slightly displaced northward with respect to the corresponding cold events that have a well configured wave pattern since 5 days previous to the event (Fig. 2). On the leeward side of the positive anomaly there is a northeasterly negative wind anomaly, extending to the northeast of the continent, which is part of the subtropical wave train, and another anomaly, although not significant, of the same sign located towards the southeast of the continent over the Antarctica peninsula (Day −4). These

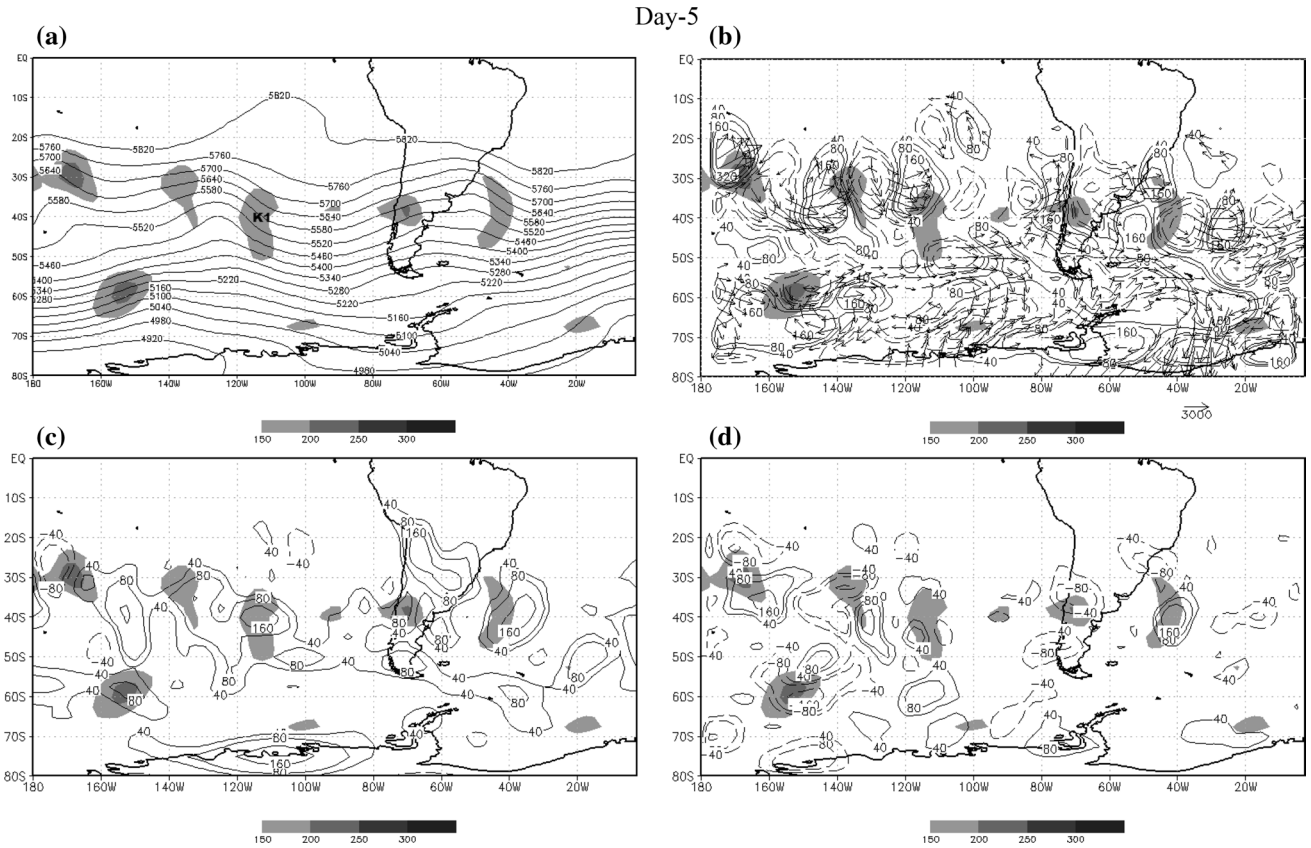

Fig. 5 For cold composite to Day −5: **a** 500 hPa geopotential height isolines (m) (*continuous lines*), **b** vertically averaged AFC term [continuous (positive) and *dashed thin* (negative) *lines*. Values plotted are 2, 7, 15 and 25 × 10^2 m^2 s^{-2}. Day^{-1}]. The vectors represent the ageostrophic flux. **c** vertically averaged BRC term [continuous (positive) and *dashed thin* (negative) *lines*, contour interval 2 × 10^{-2} m^2 s^{-2} Day^{-1}, zero omitted] and **d** vertically averaged BRT term [continuous (positive) and *dashed thin* (negative) *lines*, contour interval 2 × 10^{-2} m^2 s^{-2}. Day^{-1}, zero omitted]. Vertically averaged eddy kinetic energy (m^2 s^{-2}) is *shaded* in all *panels*

anomalies merge in a unique anomaly that strengthens during the following days reaching similar values as those of the cold events (Fig. 3). Some authors showed this characteristic associated with the extreme temperature events in the southeast of Brazil. Fortune and Kousky (1983) and Vera and Vigliarolo (2000) showed a short wave trough at higher latitudes that reaches the subtropics and facilitates the cold air outbreak into the South Atlantic Ocean and thus leading to frosts over southern Brazil. Additionally, Vera and Vigliarolo (2000) found that the strongest cold-air invasions into South America tropical regions strongly depend on the presence of an upper level subtropical cyclonic perturbation. In this way, PA05 highlights the fundamental role of the cyclone off the Brazilian coast as a dynamic mechanism for the formation of frosts in southeastern Brazil.

It is proper to do an analogy with the results of Müller and Berri (2007, 2012) for the most persistent frost days in central-northern Argentina, for which they showed that the wave patterns driven by the corresponding jets were coupled to the west of the continent, windward to the Andes Mountains. Therefore, both wave train phases, subtropical and sub-polar, coincided prior to the event, continuing with zonal propagation even after the event. Similar to what is shown here, two wave trains couple before the event but in this case on the east of the continent, leeward to the Andes Mountain, and then continue to follow a more zonal propagation in comparison with cold events, although the sub-polar wave train is statistically no confident. In the same way as shown by Müller and Ambrizzi (2007) for the basic state leading to a higher frequency of frosts occurrence in the Wet Pampa.

From a synoptic point of view, this upper-level wave pattern is associated with the passage of a cold front with a predominantly zonal trajectory in low levels and with an intense low pressure system in the south–southeast part of the continent (figure not shown), as obtained by Escobar (2007) in the third EOF mode of the synoptic patterns of cold waves in the region of Sao Paulo. The main characteristic of this circulation pattern is the rapid west-east movement of the post frontal anticyclone (Escobar 2007) entering the continent at lower latitudes when compared to the cold frost events. This allows the cold air mass to be preserved in its eastward trajectory, which contributes to its

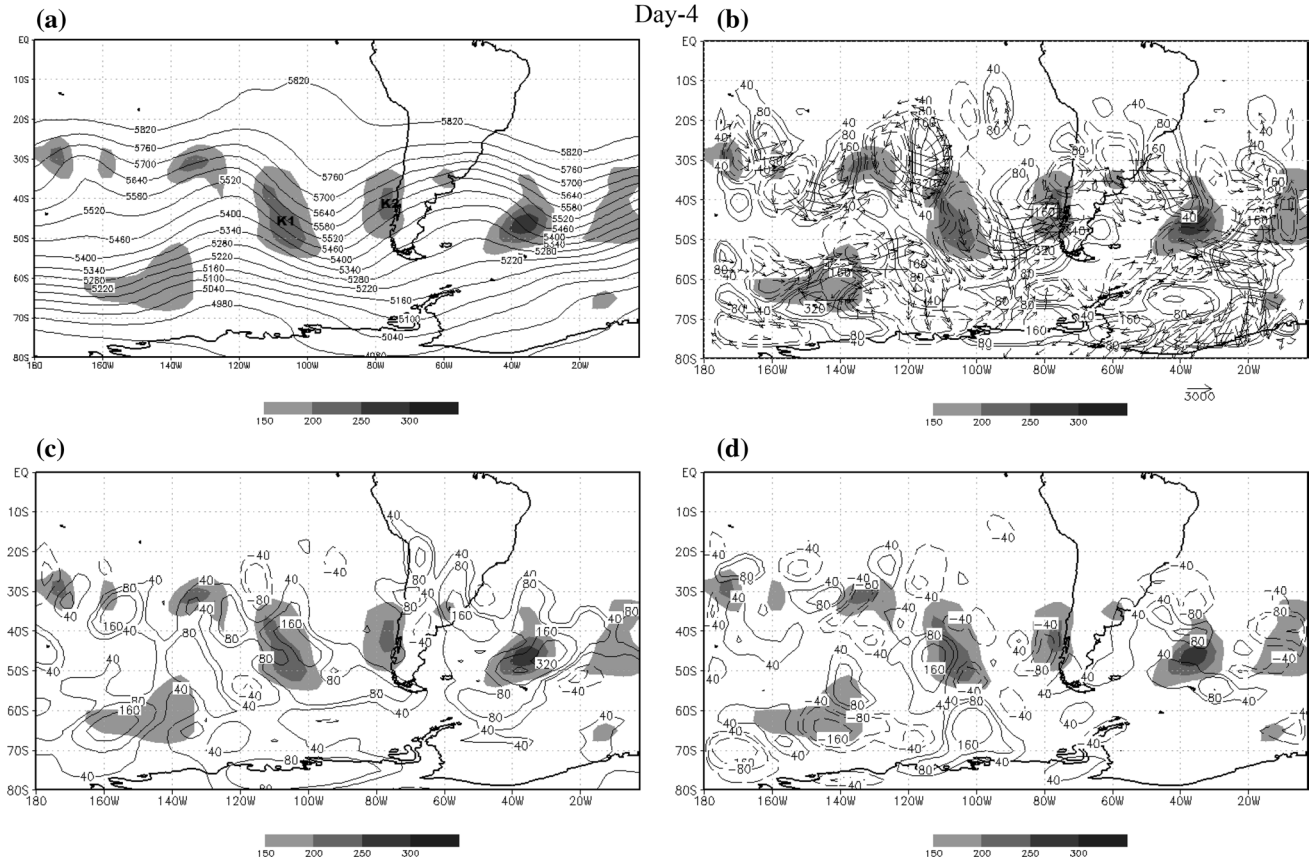

Fig. 6 As Fig. 5 for Day −4

having a southern wind along the lee side of the Andes, and in keeping with its continental characteristics which favor an intensified nocturnal radiative loss, which in effect will lead to lower minimum temperatures.

3.3 Individual events

In order to clarify the patterns obtained from the cold and cool composite analysis, some individual events are discussed here. Figure 4a shows the Day −1 propagation pattern associated with a cold event which took place in São Paulo on June 1st, 1979, where only one wave train at 300 hPa, propagating from the Pacific towards the Atlantic Ocean, was able to affect a large part of the continent. Figures 4b, c give two examples of cool events which took place on June 27th, 1994 and July 7th, 1975, respectively. One should notice that the propagation patterns at 300 hPa are quite similar to those of the composites of Fig. 3, suggesting that the latter captures many of the features of the individual cases. These examples show the wave train zonal propagation which in previous days appears divided in two (figures not shown), one at subtropical latitudes and the other propagating along polar latitudes. On the day previous to the event, they merge into only one pattern over the Atlantic Ocean, which is responsible for the surface cooling observed on the following morning in tropical latitudes.

4 Energtics of wave train propagation

4.1 Cold frost events

The vertical integrated kinetic energy evolution for the cold event composite (Figs. 5, 6, 7, 8, 9, 10, 11) shows many energy maxima around the western Southern Hemisphere on Day −5 (Fig. 5a). The kinetic energy maximum at 115°W–40°S (K1) is associated with a 500 hPa trough upstream (Fig. 5a) and the 300 hPa meridional wind negative anomaly (Fig. 2a) that propagates slowly to the east, associated with the cold frost event. On Day −4, other energy maximum (K2) developed downstream of K1 at 78°W–40°S (Fig. 6a). Both maxima are associated with the ridge over the eastern South Pacific, where K1 is upstream of the 500 hPa ridge axis and K2 downstream. On Day −2, other energy maximum (K3) developed over the South

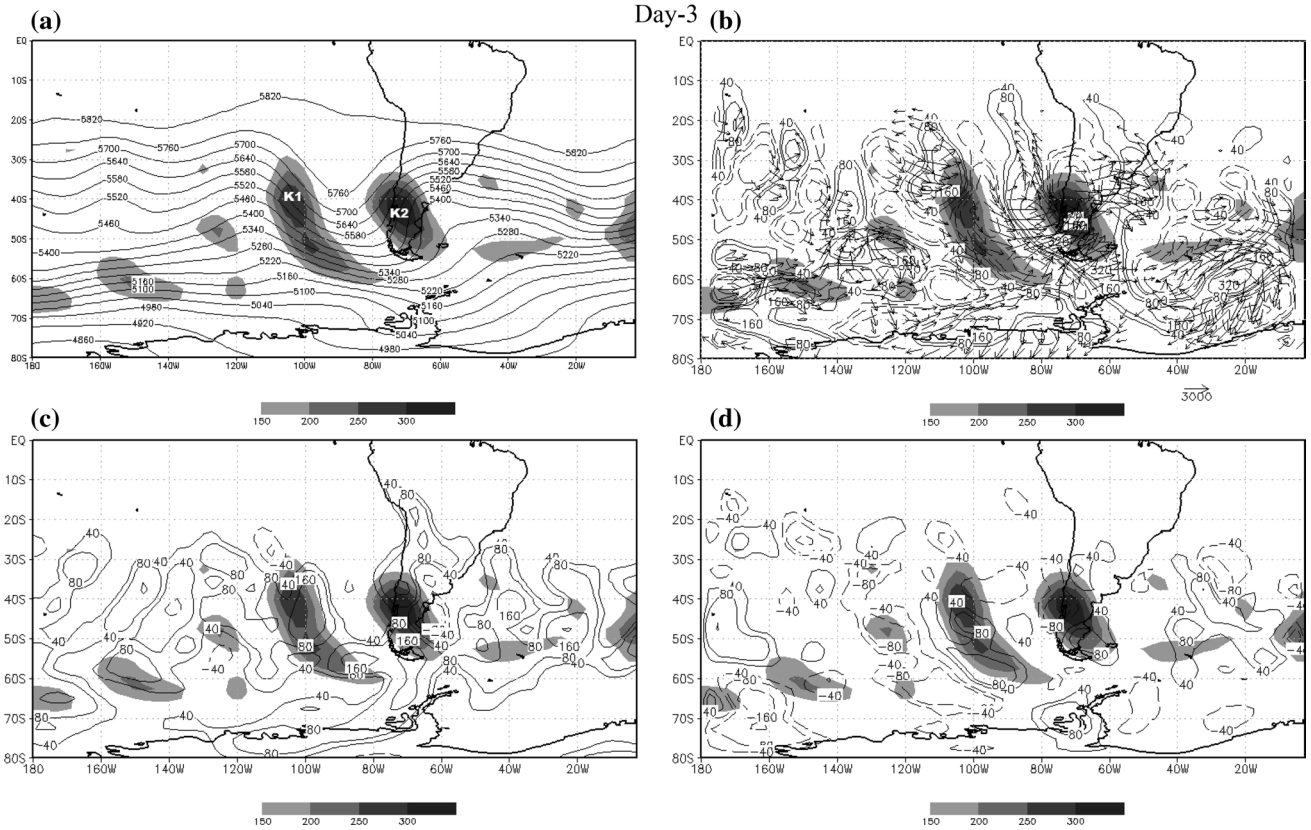

Fig. 7 As Fig. 5 for Day −3

Atlantic close to the southern Brazil coast (40°W–37°S) (Fig. 8a). These three maxima continued to be stationary until Day −1 (Fig. 9a) when K1 dissipated and the K2 and K3 maintained their magnitude. On this day, these two energy centers are associated with a trough located to east of the coast of southern Brazil. On Day 0 (Fig. 10a), K2 is very weak and K3 begins the decaying phase, persisting over the South Atlantic until Day +1 (Fig. 11a).

It can be seen that K1 had positive BRC and BRT on Days −5 (Fig. 5c, d, respectively), being the baroclinic more intense. On the other hand, the AFC term had positive contribution (importing energy) in the northern sector of K1 and negative (exporting energy) in the southern sector of K1, but one can see that more energy was imported than exported.

On Day −4, BRC continues to dominate the region of K1 (Fig. 6c) and AFC is acting positively only in the northwestern sector of K1, while it isnegative over the rest of the maximum and divergence of this flux domains almost of the K1 region (Fig. 6b). The barotropic term has positive values around the central sector of K1 and negative in northern and southern sector. For K2 on this day, there is no significant baroclinic contribution throughout the K2 region (Fig. 6c) but convergence of ageostrophic fluxes in the southwestern sector of this energy maximum and divergence in northeastern (Fig. 6b) is observed. On the other hand, BRT has a negative contribution throughout the central-western sector and a positive one throughout the northern and southern sectors. In this case, the main mechanism to the initial development of K2 is the AFC. The reason for this development is the fact that kinetic energy imported upstream is higher than the energy exported downstream.

On Day −3 the situation for K1 is very similar to that of Day −4, but the convergence of ageostrophic flux is higher than on Day −4 exactly in the region of K1. On the other hand, divergence of this flux dominates large regions of K1. In K2 the convergence of ageostrophic flux in the western sector and divergence in northeastern sector become larger than on Day 4. Other AFC center is formed downstream of K2 (Fig. 7b) where K3 develops on Day −2 (Fig. 8a). The baroclinic term is positive in the large area of K2 (Fig. 7c) and the barotropic term shows positive and negative conversion (Fig. 7d), so that these conversions intensify K2 on Day −2.

During Day −2 (Fig. 8) there are positive baroclinic contributions to the K1 region (Fig. 8c), convergence of ageostrophic flux in the northwest sector of K1, export of kinetic energy along the remainder area of K1 (Fig. 8b),

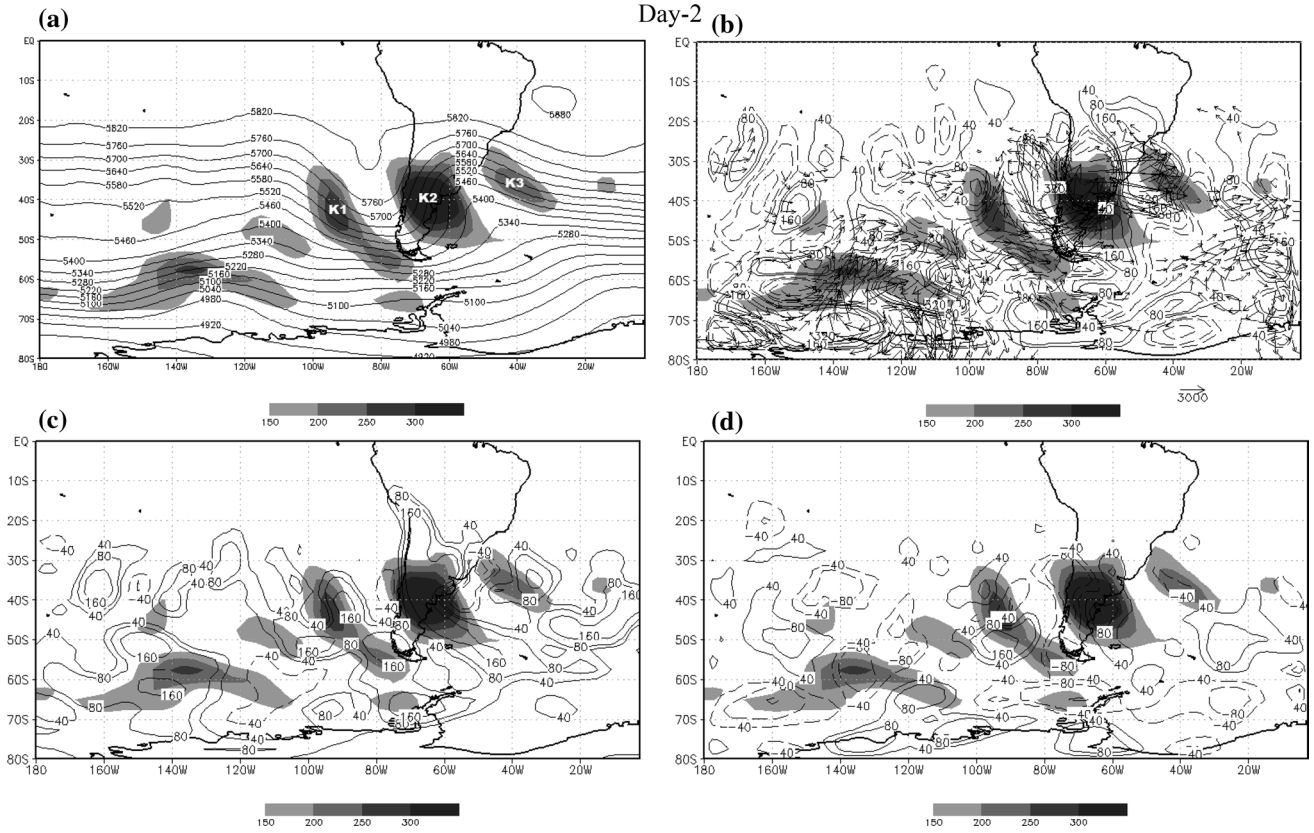

Fig. 8 As Fig. 5 for Day −2

and positive and negative BRT (Fig. 8d). This situation contributes to K1 and becomes weak over southern of South America on Day −1 (Fig. 9a). For the K2 on Day −2, the BRC is positive (Fig. 8c), BRT is negative in western sector and positive in eastern sector (Fig. 8d), so BRT does not contribute to weaken or intensify this energy center. Kinetic energy is imported by AFC in the western boundary of K2 and exported downstream to K3 in most of the K2 area (Fig. 8b), so more K′ is exported than imported by this term, contributing to weaken K2. Throughout the most part of the K3 region negative barotropic contribution is observed (Fig. 8d) along with negative and positive baroclinic contribution (Fig. 8c) and positive values of AFC, although there is divergence of ageostrophic flux in the southern sector (Fig. 8b). This situation contributes to intensify K3 on Day −1 (Fig. 9a).

On Day −1 (Fig. 9), K1 is very weak despite the existence of positive baroclinic conversion. Over the K2 region high positive values of BRC and divergence of ageostrophic flux are observed. At the same time over the K2 area there are positive and negative contributions of BRT, and AFC and baroclinic terms have values of the same order but with opposite signs. Nevertheless, K2 weakens, which suggests that other dissipative processes also contribute to the decrease of the K2 magnitude.

During Day 0 (Fig. 10) K3 is intense with positive baroclinic and negative and positive BRT. The AFC has positive (northern sector) and negative (southern sector) values. On Day +1 (Fig. 11) K3 is weak although there is positive baroclinic conversion.

The time evolution of K′ as well as AFC, BRC, BRT and KFC conversion terms integrated through the volume represented by the box in Fig. 1a–c for the kinetic energy maxima K1, K2 and K3 are shown in Figs. 12, 13 and 14, respectively. The other Eq. 2 terms are not shown in these figures because they are small, although they are used to calculate the RES term. For K1 (Fig. 12) one can see that K′ is increasing from Day −5 to Day -3 (positive OKT). After these days, K′ decreases (negative OKT), reaching its minimum on Day −1, when it increases again. During the first K′ intensification phase of K1, the AFC and KFC are initially positive but with opposite tendency, while BRC is increasing and AFC is negative. Comparing the K′ with BRC term evolution one can see that both show the same behavior, although BRC reaches its maximum about 12 h later. After Day −4 at 0600 UTC, AFC is negative, meaning that kinetic energy is being exported out of the region

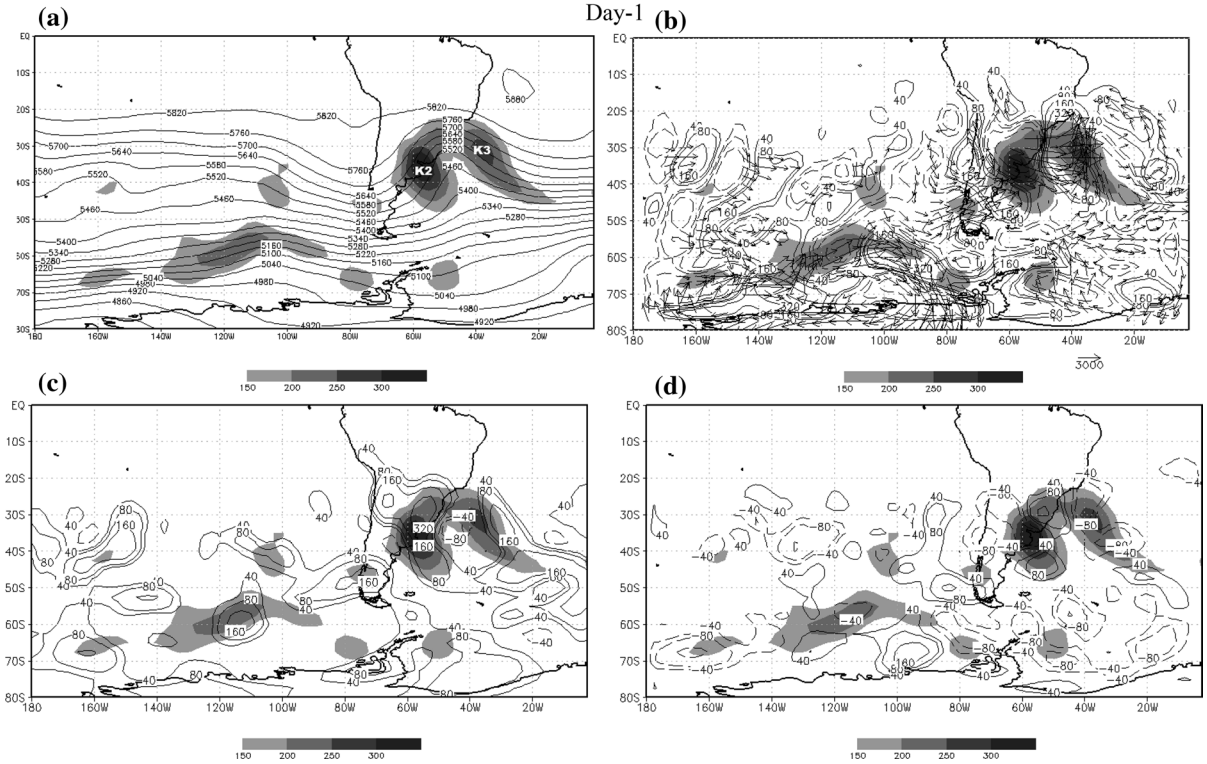

Fig. 9 As Fig. 5 for Day −1

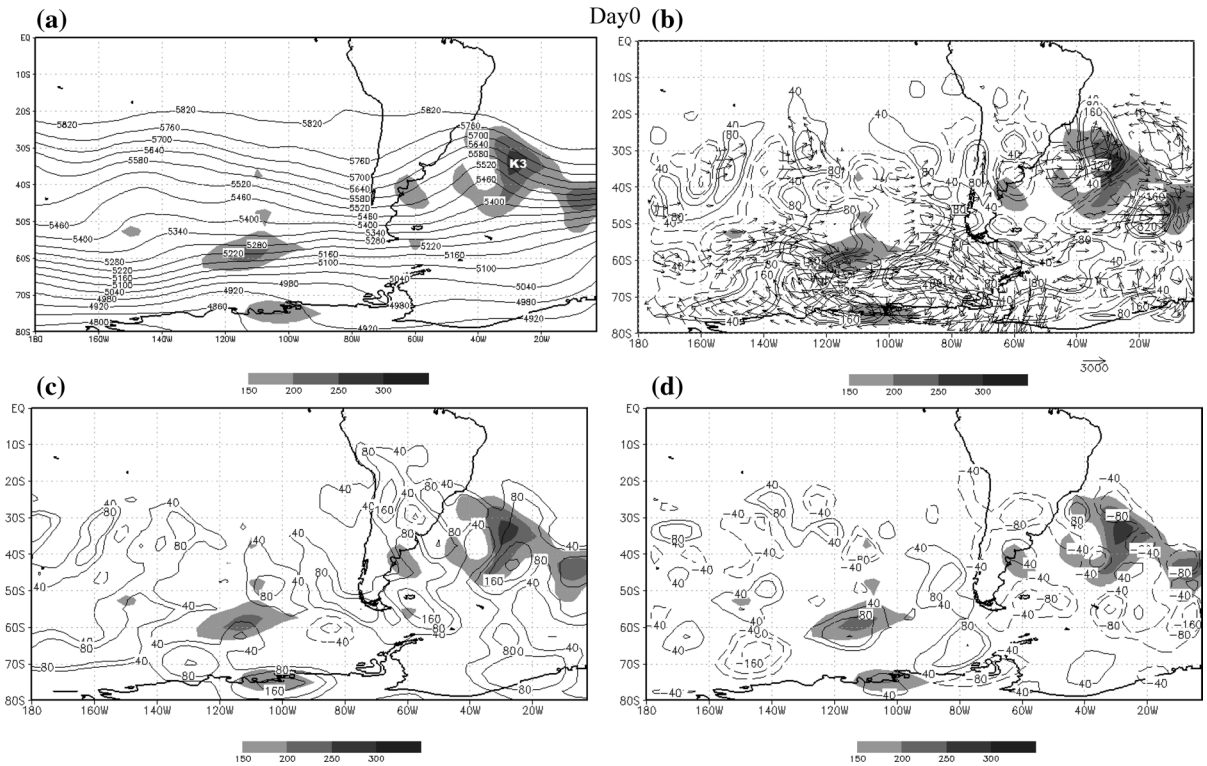

Fig. 10 As Fig. 5 for Day 0

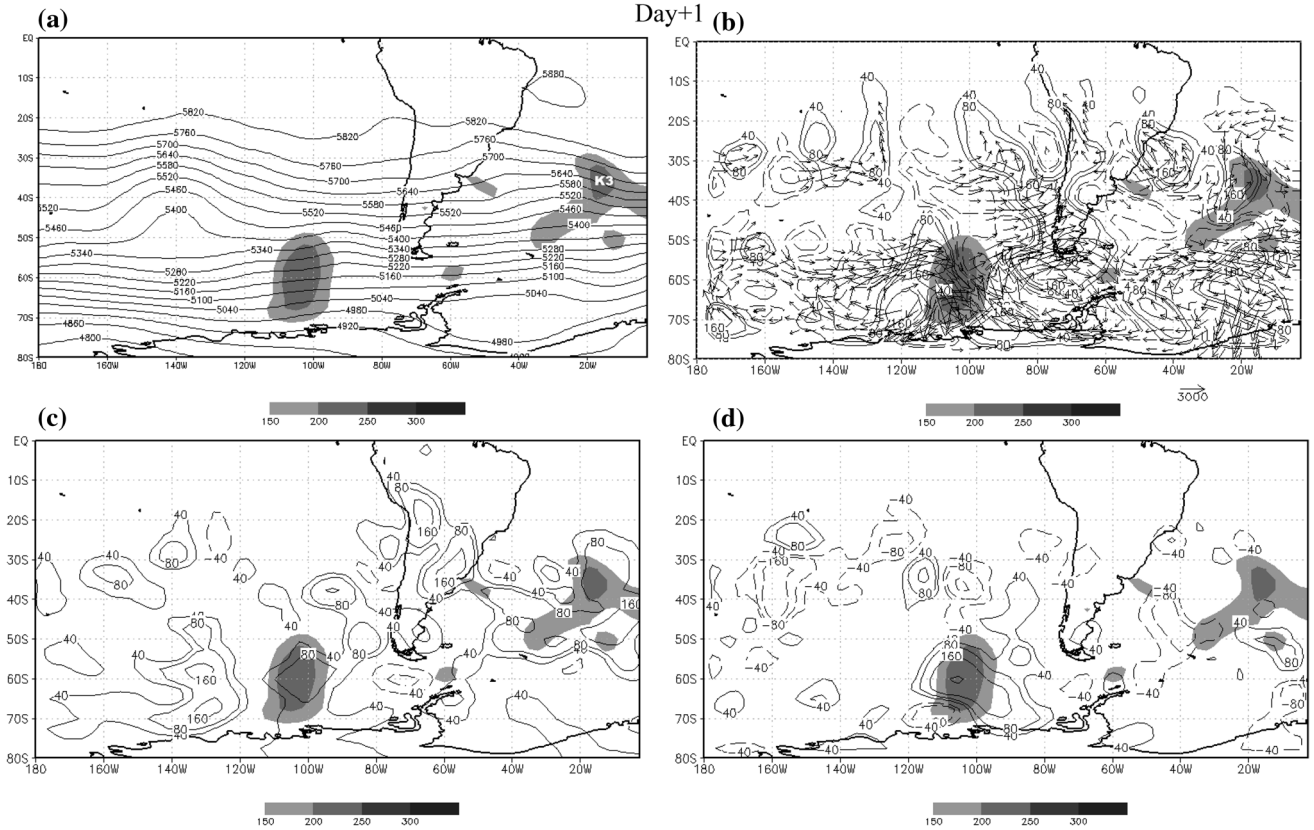

Fig. 11 As Fig. 5 for Day +1

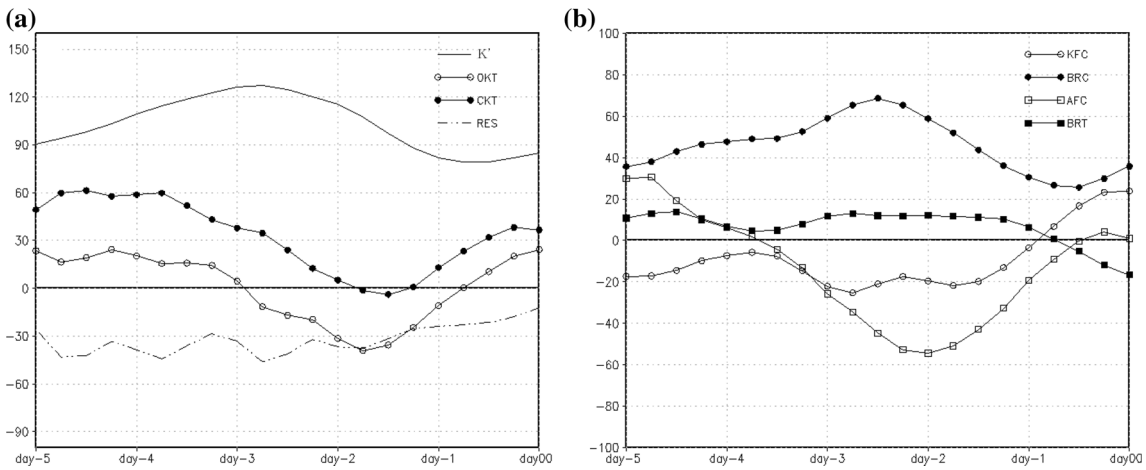

Fig. 12 Temporal evolution of volume-averaged **a** K′ (*solid line*), OKT (*open circles*), CKT (*closed circles*) and RES (*dotted-dashed line*) (*left panel*), **b** KFC (*open circles*) BRC (*closed circles*), AFC (*open squares*), BRT (*closed squares*) for K1. Units are $m^2\ s^{-2}\ Day^{-1}$, except for K′ unit which is $m^2\ s^{-2}$

K1. The BRT term is positive until Day −1 at 0600 UTC but its contribution is small compared to the BRC term. The RES term is negative all the time, meaning that other dissipative mechanisms could have been acting, such as friction and other diabatic effects. As the KFC term only contributes to displace the K′ center because it is associated with advective flux (Chang 2000), it is not important regarding the intensification of the waves. Thus, the BRC

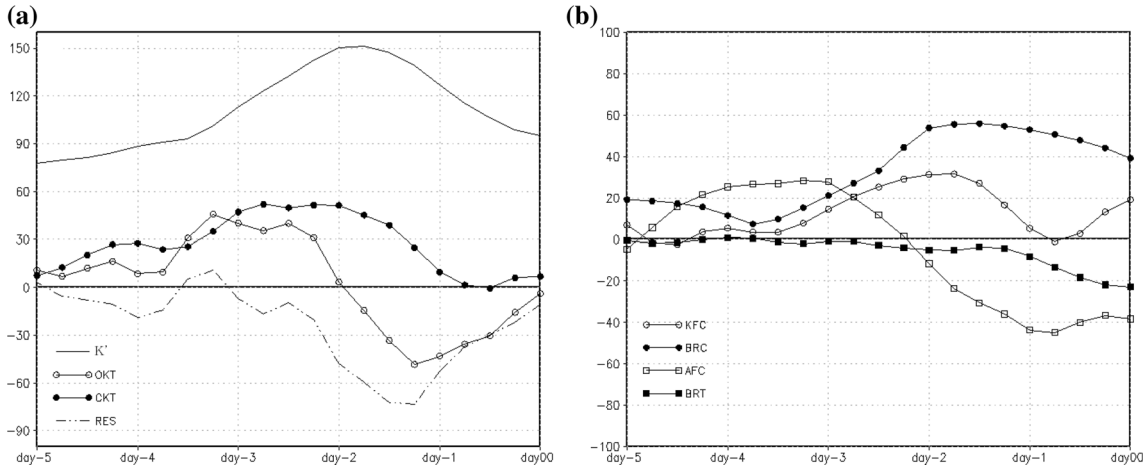

Fig. 13 As Fig. 12 for K2

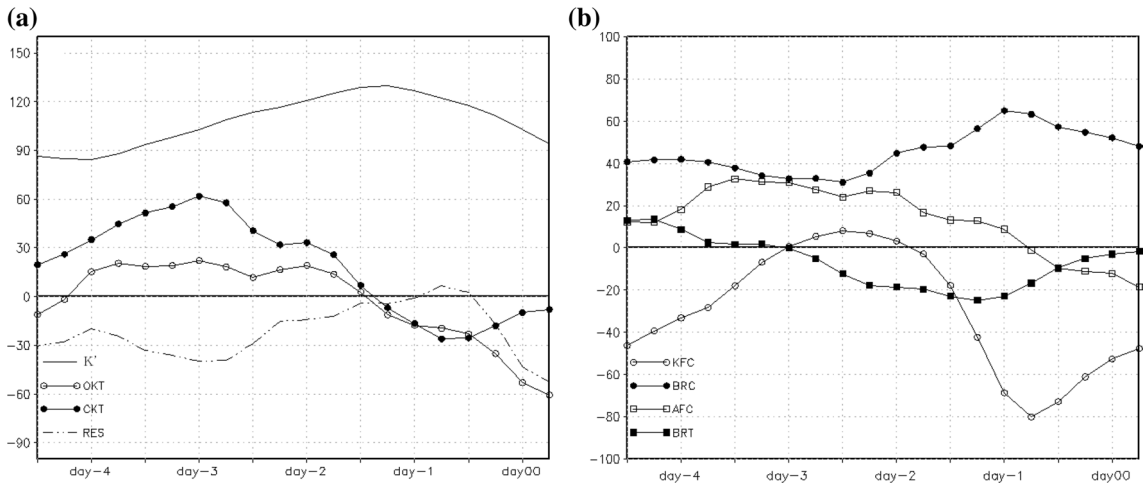

Fig. 14 As Fig. 12 for K3

instability is the most important mechanism to increase the kinetic energy in K1, while AFC exports K′ to K2.

K2 develops from Day −5 to Day −4 and during Day −5, the region of K2 has a positive contribution from BRC and AFC terms (Fig. 13b), although BRC reduces its values while AFC increases. During the maximum intensification of K2 (from Day −4 at 12 UTC until Day −2) the BRC term grows reaching its maximum value at the same time that K′ reaches its maximum. On the other hand, the AFC term is maximum from Day −4 to Day −3, and during Day −3 AFC decayes, reaching its minimum on Day −1. The BRT term is negligible until Day −2, after which the BRT conversion has a negative contribution. As in the case of K1, in K2 the RES term is also negative throughout almost the entire period, but in this case the RES is small at the initial phase. After Day −2 it becomes increasingly negative, meaning that during this period other dissipative mechanisms could have been present. Thus, AFC has an important role in the initial phase of K2 development and BRC conversion after Day −3. The K2 development is similar to the Downstream Baroclinic Development (DSBD) theory proposed by Orlanski and Sheldon (1995). In this theory an upper level wave develops by receiving K′ from an upstream wave, and when this wave intensifies at surface, cyclones can form. The wind circulation associated with this cyclone contributes to intensify the baroclinic zone, after which the cyclone intensifies by baroclinic conversion.

Over the region where K3 develops, a minimum value of K′ is present on Day −4 that reaches a maximum on Day −2 at 1800 UTC (Fig. 14). During this period, the BRC term has a positive contribution, but after Day −3 at 1200 UTC this term increases its contribution reaching a

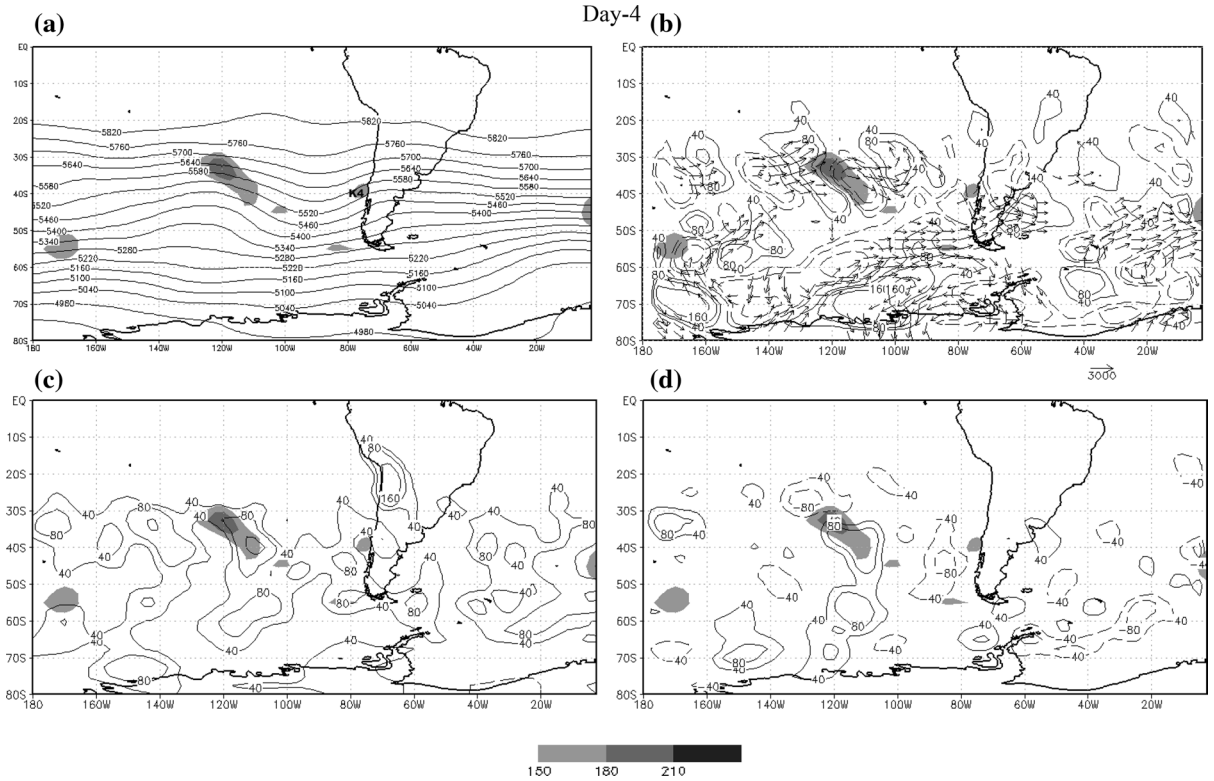

Fig. 15 As Fig. 5 for cool composite and Day −4

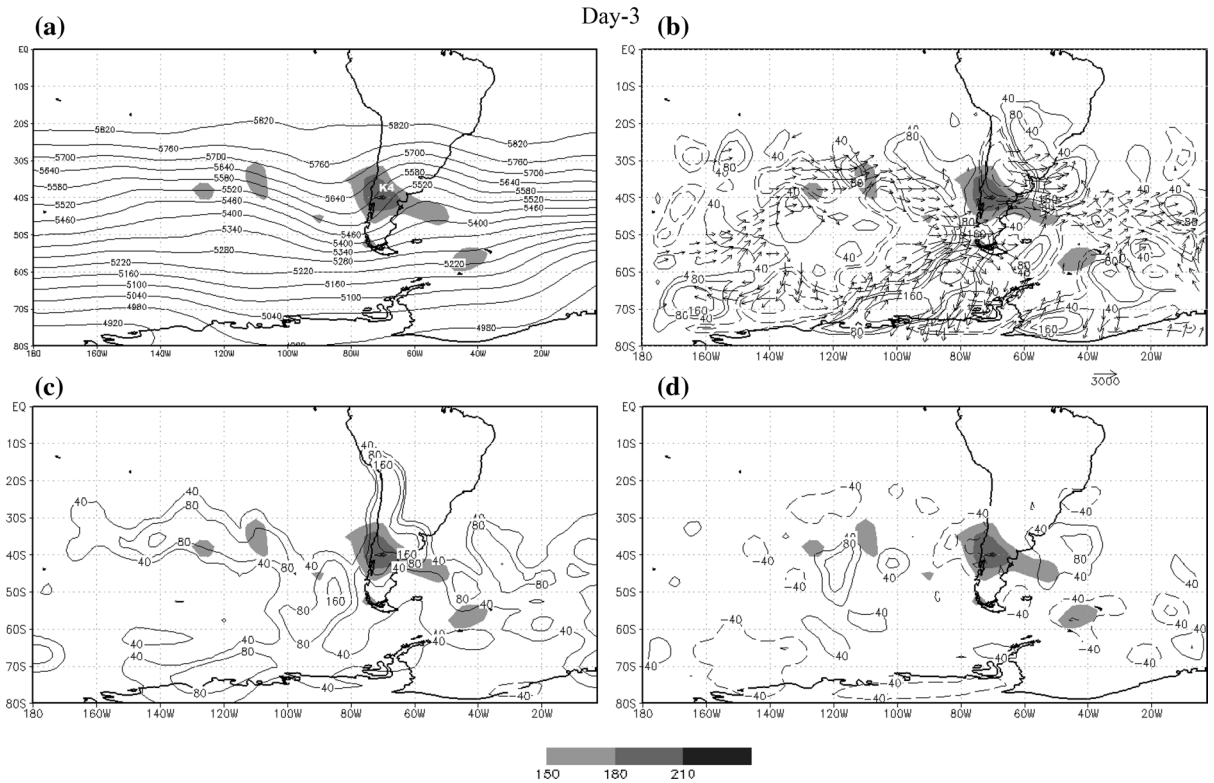

Fig. 16 As Fig. 15 for Day −3

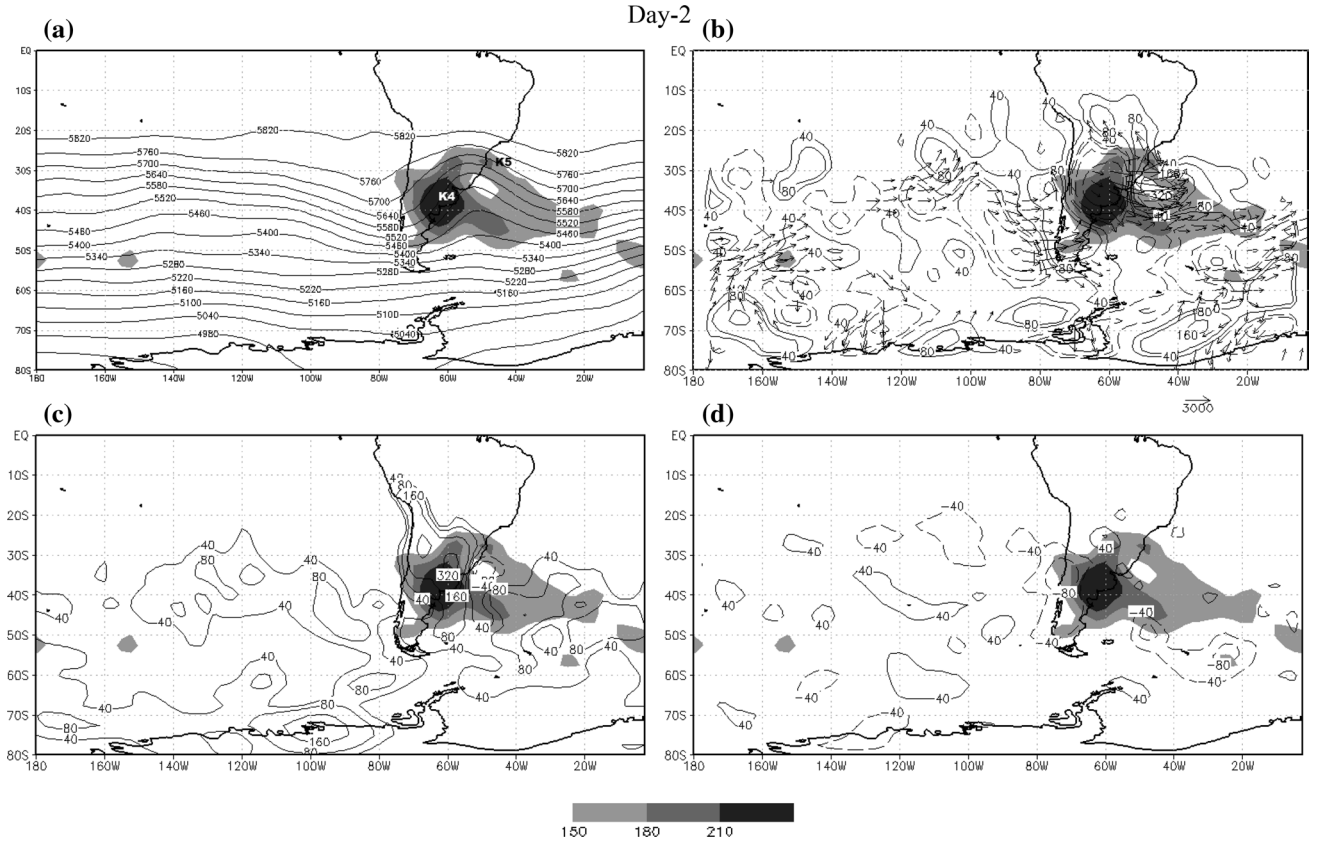

Fig. 17 As Fig. 15 for Day −2

maximum on Day −1. K′ is imported in K3 region by the AFC term since Day −4 until Day −1, but its contribution is smaller than that of the BRC term, which is negative after Day −3, meaning that K′ is converted to basic state kinetic energy. In this case RES is also negative, although in a different way than in the case of K2 since RES has large negative values at the initial phase and then they become small after Day −2.

The evolution of K1 and K3 is similar to the 1B and 1C trough studied by Chang (2000) and to the cyclogenesis type B of Piva et al. (2010) which during their initial growth phase, the baroclinic and the convergence of ageostrophic flux make a contribution, and the decay phase is dominated by ageostrophic flux divergence mainly in K1. The evolution of K2 coincides with the results of Orlanski and Sheldon (1995) who observed that baroclinic wave developments are frequently associated with the convergence of ageostrophic flux, i.e., the development of this wave is extracting energy from upstream mature perturbations rather than from the mean flow, while in the decay phase the divergence of ageostrophic flux dominates, although for K2 there could other important dissipating mechanisms.

4.2 Cool frost events

In contrast to the cold frost event composites, the vertical integrated kinetic energy evolution for the cool event composite (Figs. 15, 16, 17, 18, 19, 20) shows only three energy maxima around the western Southern Hemisphere on Day −4 (Fig. 15a). These maxima are less intense than in the cold frost composites and just one K4 maximum energy located at the Chilean coast around 40°S, downstream of an intense 500 hPa ridge over South Pacific around 95°W and upstream of a weak 500 hPa trough over Argentina, is associated with the cool frost over São Paulo State. K4 has positive and weak BRC (Fig. 15c), and the divergence of ageostrophic flux is also observed at the east and west of this center (Fig. 15b).

On Day −3 (Fig. 16), the wave (the ridge and the trough) amplifies and K4 intensifies and expands to the east over central region of Argentina (Fig. 16a). The baroclinic conversion increases over the K4 region (Fig. 16c), and positive AFC (Fig. 16b) and negative BRT (Fig. 16d) are present to the west of K4. A region of negative AFC is developing in the area downstream of the convergence region of this flux and another region of positive AFC is

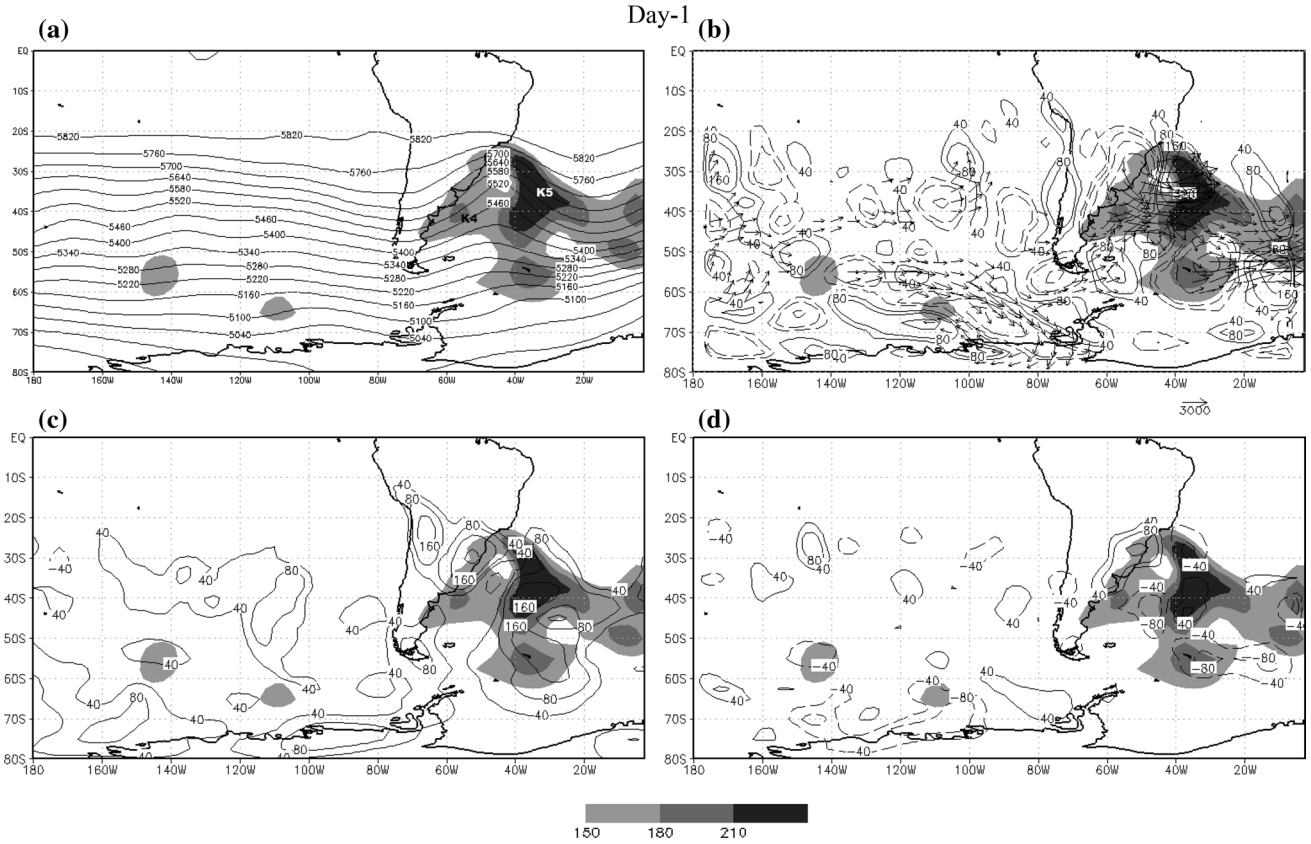

Fig. 18 As Fig. 15 for Day −1

formed in the area downstream of the ageostrophic flux divergence region.

The K4 and the wave continue propagating to the east, and on Day −2 (Fig. 17a) they are over the central-east region of Argentina. During this eastward displacement K4 and the trough intensifies, in association with large values of baroclinic conversion (Fig. 17c). Part of the energy of K4 is exported to east by the ageostrophic flux as one can see the large area of intense divergence of this flux over the K4 region (Fig. 17b). A region of positive AFC to the east of K4 continues developing. Over this region, the kinetic energy is increasing and a new energy maximum (K5) is observed, which is also associated, to the West, with a small positive baroclinic conversion and, to the South, with negative baroclinic conversion (Fig. 17c).

During Day −1, K4 is very weak and is associated with ageostrophic flux divergence (Fig. 18b) and positive baroclinic conversion (Fig. 18c). On the other hand, K5 is intensifying by AFC and positive baroclinic conversion. On this day, three secondary kinetic energy maxima appear, one to the South of the K5 and another two over the Pacific Ocean, one around 110°W–63°S and the other one around 145°W–55°S.

On Day 0, K5 continues to be intense, associated with positive baroclinic conversion (Fig. 19c), and positive (western sector) and negative (eastern sector) values of AFC (Fig. 19b). On Day +1, K5 is far from the continent, weak and associated with positive baroclinic conversion (Fig. 20c) and ageostrophic flux divergence (Fig. 20b). During this period, barotropic contribution is small and normally negative such as for K4 and as for K5.

The time evolution of K′ and the conversion terms integrated through the volume (Figs. 21, 22) represents by the box showed in Fig. 1d, e for the kinetic energy maximum K4 and K5, respectively, shows that K4 intensifies prior to Day −4 until Day −2 (positive OKT), when it reaches its maximum value. During this period K4 develops basically by baroclinic conversion because the BRT term has a very small contribution and the AFC just extracts K′ from K4 (Fig. 21). In decay phase (after Day −2) the ageostrophic flux continued extracting K′ and the BRC term reduces its positive contribution. On the other hand K5 develops from Day −4 at 1200 UTC to Day −1 (positive OKT) by AFC and baroclinic positive conversion, although it decays by ageostrophic flux divergence (Fig. 22). The BRT term is small during all the period. As in the cold frost composite,

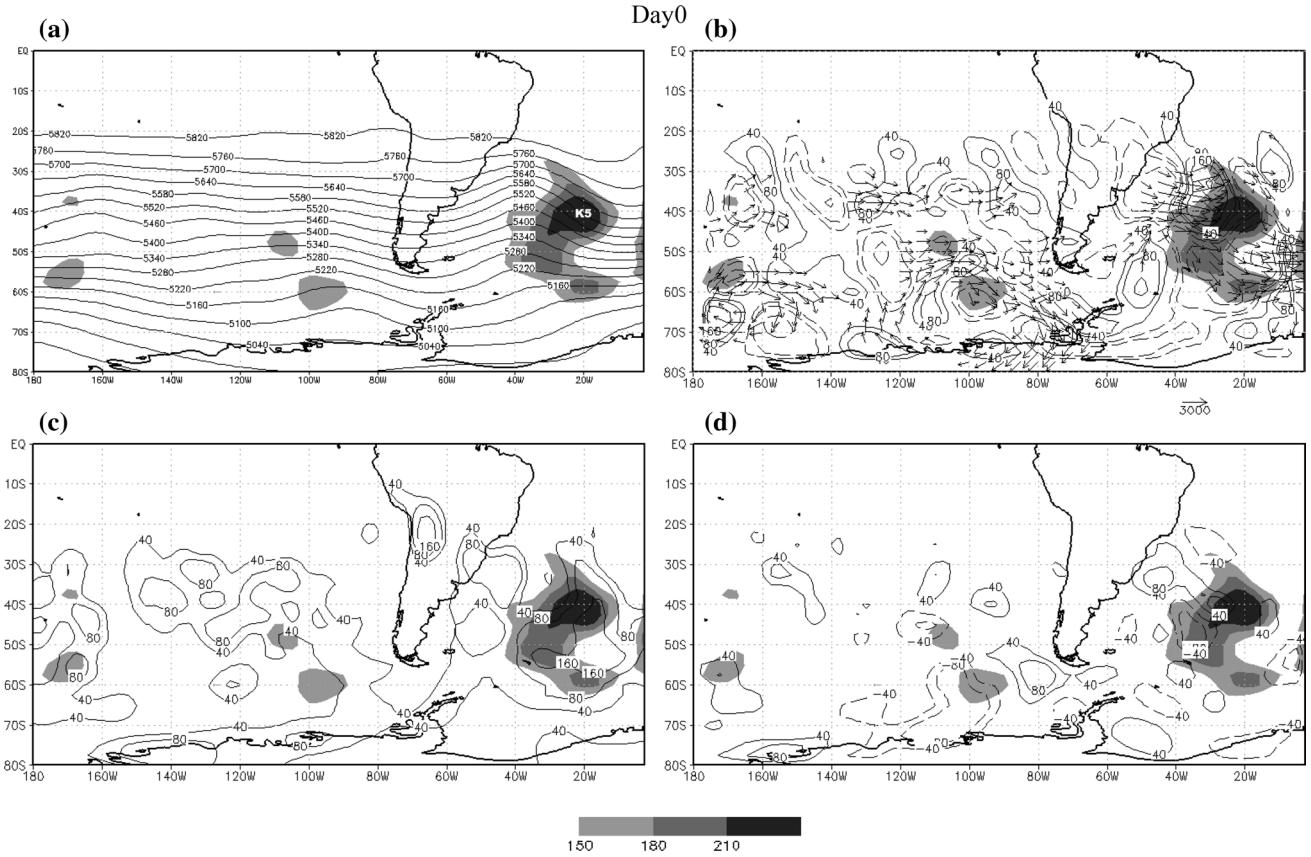

Fig. 19 As Fig. 15 for Day 0

the RES term is negative, although in this composite the negative K4 and K5 values are small.

5 Discussion and conclusions

Through the composite analysis of cold and cool frost events which affect the tropical latitudes of South America, the differences in the propagation patterns which drive the atmospheric circulation were investigated. Considering the dynamics and the energetics of the wave train propagation associated to such events, the observed differences related to the intensity of the cold air incursion are discussed.

The cold events are associated with a single wave pattern with propagation along the Pacific Ocean and moving towards South America, with an arc-like trajectory which ends in the Atlantic Ocean. This is the classical trajectory followed by the most intense events reaching these latitudes and they have been extensively documented. However, this is not the only type of propagation that can lead to a frost. The cool events are associated with a subtropical wave pattern that propagates along the Pacific Ocean, which merges with another wave, although not significant, coming from polar latitudes of the western Atlantic Ocean before the event, similar to what Vera and Vigliarolo (2000) showed, and then continues to the east in a basically zonal propagation.

The differences in the wave propagation patterns between the two types of events analyzed here may explain their observed intensity. Cool events are associated with zonal patterns which move the low level anticyclone from the southwest of the continent (located further north than the cold events) to tropical latitudes. This anticyclone is strengthened together with the meridionaly extended cyclone located upstream. This configuration causes southerly wind advection over all the central-southeast Brazil, and consequently the observed temperature decrease at tropical latitudes. This system is less intense than in the cold events, which is consistent with the results presented by Pezza and Ambrizzi (2005) showing that wind at low levels for the cool frost events has half the intensity over the continent than that of the composites of cold frost events. The results obtained reflect what was described by the propagation patterns. Therefore, in the cold (cool) events it is observed a meridional (zonal) trajectory leeward to the Andes Mountain, particularly for the surface anticyclone. This meridional trajectory is resulted by the interaction between the topographic wave and the anticyclone (Gan and Rao 1994).

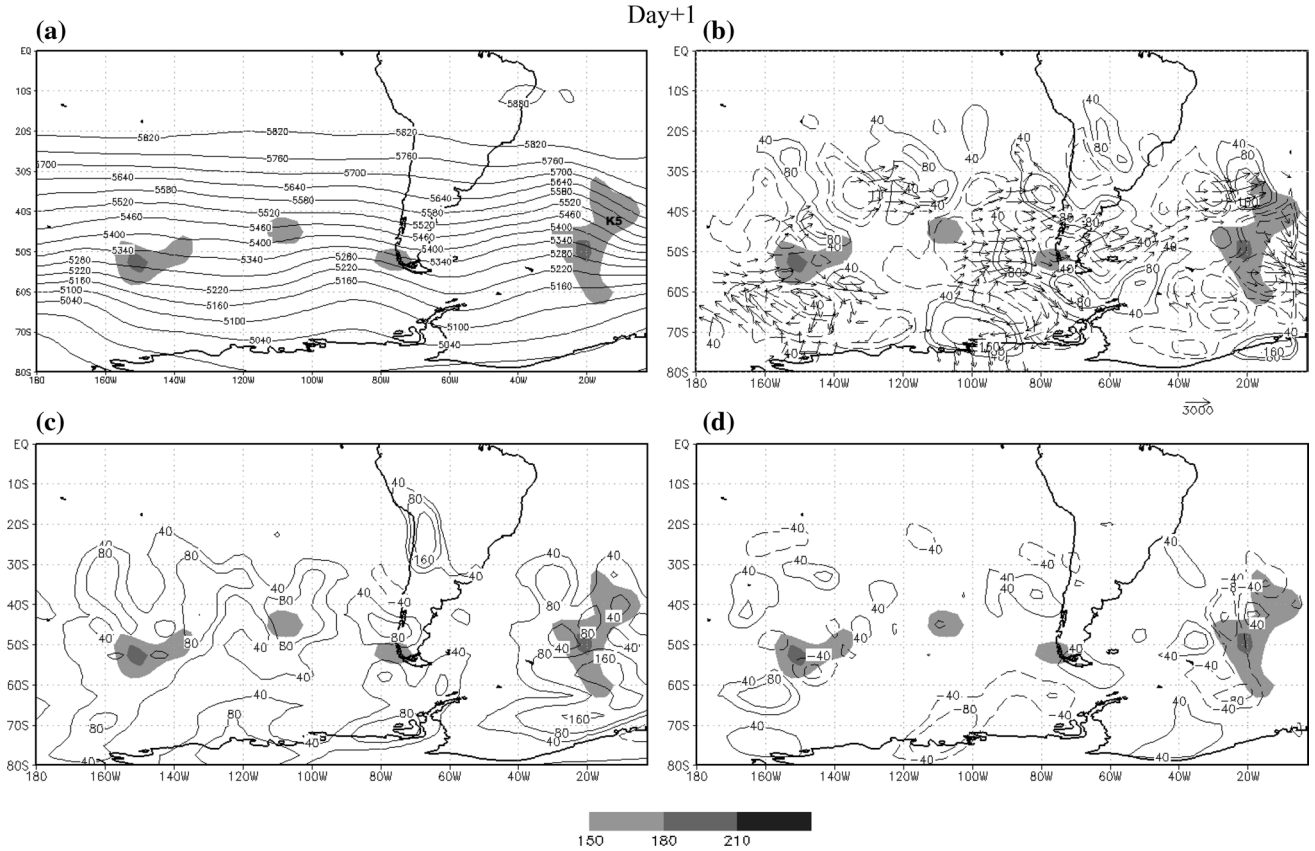

Fig. 20 As Fig. 15 for Day +1

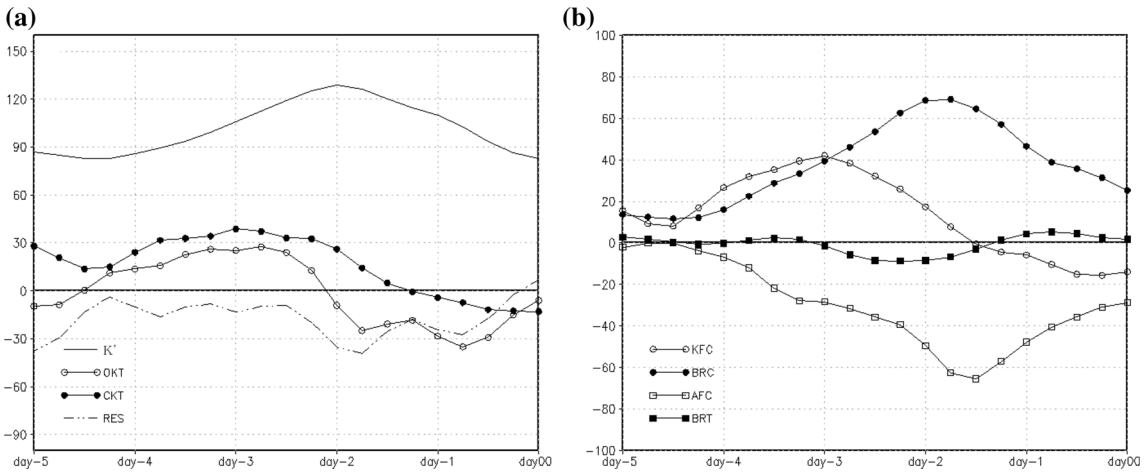

Fig. 21 As Fig. 12 for K4

The energetics shows some important difference between the cold and cool frost events. For the cold events the energy maxima are more intense than in cool events. Three kinetic energy maxima (K1, K2 and K3) are observed to be associated with the wave that causes the cold event. The initial phase of K1 and K3 maxima is associated with baroclinic conversion and ageostrophic flow convergence, while K2 is only with ageostrophic flow convergence. The decay phase of these three maxima is associated with ageostrophic flow divergence, although other dissipating mechanisms could be acting to weaken these energy maxima. In some of the days of these kinetic energy maxima, the RES

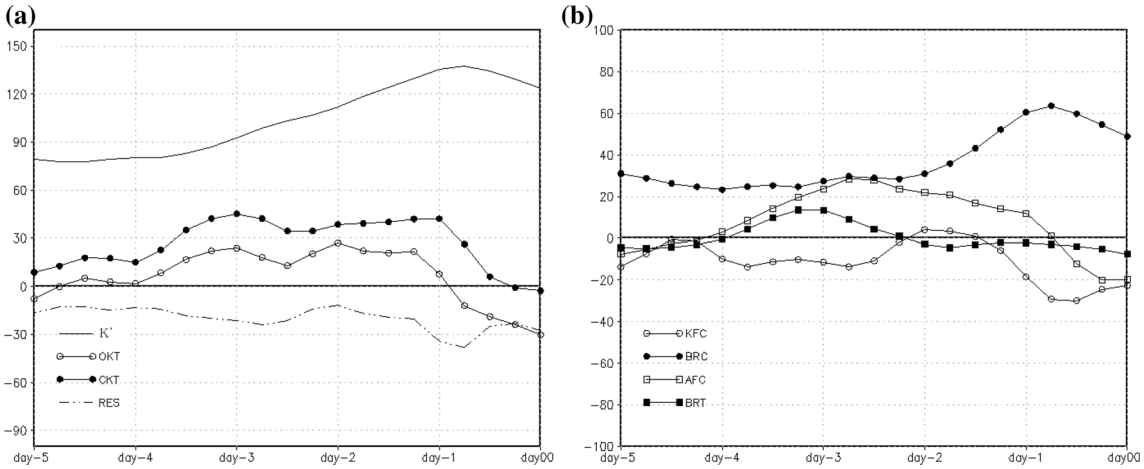

Fig. 22 As Fig. 12 for K5

term has the same order of magnitude than the individual terms. Part of the RES term error is because of the errors introduced by numerical methods and sub-grid fluxes, but as it is always negative, some dissipative mechanisms (that are not present in the equation) could also be acting, such as diabatic heating and friction. Garreaud and Fuenzalida (2007), based on numerical results, concluded that diabatic heating associated with latent heat release plays an important role in the upper tropospheric cyclonic vortex dissipation when this system is over Eastern South Pacific Ocean. As the RES term has the same order of magnitude than the individual terms just during some days, it means that during these days dissipative mechanisms were present. The RES term was most of the time negative, indicating that other kinetic energy dissipation mechanism is not present in the equation. The inclusion of friction would probably reduce the CKT term, making it more approximated to the OKT term, and eventually reducing the RES term to one order of magnitude smaller than the main forcing terms. The decay phase of these two maxima is associated with ageostrophic flux divergence.

For the cool events, two maxima of kinetic energy (K4 and K5) are observed with the wave that causes the frost event. The K4 formation and intensification phases are associated with baroclinic conversion and K5 with ageostrophic flux convergence and baroclinic conversion. The decay phase of these two maxima is associated with ageostrophic flux divergence. For these two maxima, the RES term is smaller than the individual terms, but it is negative as it occurred with the cold events kinetic energy maxima.

Thus, in both types of frost events, the intensification of the wave is associated with ageostrophic flux convergence. Our results are in agreement with Krishnamurti et al. (1999) results for the major frost events that have occurred over southeastern Brazil, when downstream amplification of the wave train prior to the frost event, associated with ageostrophic flux convergence, is observed.

Acknowledgments This work was partially supported by grants PICT-PRH 0023 from ANPCyT (Agencia Nacional de Promoción Científica y Tecnológica). The authors acknowledge the useful comments and suggestions made by the anonymous reviewers that contributed to improve this paper.

References

Chang EKM (2000) Wave packets and life cycles of troughs in the upper troposphere: examples from the Southern Hemisphere summer season of 1984/85. Mon Weather Rev 128(1):25–50

Escobar GCJ (2007) Padrões Sinóticos Associados a ondas de frio na cidade de São Paulo. Revista Brasileira de Meteorologia 22(2):240–253

Fortune M, Kousky VE (1983) Two severe freezes in Brazil: precursors and synoptic evolution. Mon Weather Rev 11:181–196

Gan MA, Rao VB (1994) The influence of the Andes cordillera on transient disturbances. Mon Weather Rev 122(6):1141–1157

Garreard and Fuenzalida (2007) The influence of Andes on cutoff lows: a modeling study. Mon Weather Rev 135:1596–1613

Garreaud R (2000) Cold air incursions over subtropical South America: mean structure and dynamics. Mon Weather Rev 128: 2544–2559

Kalnay E, Kanamitsu M, Kistler R, Collins W, Deaven D, Gandin L, Iredell M, Saha S, White S, Woollen J, Zhu Y, Chelliah M, Ebisuzaki W, Higgins W, Janowiak J, Mo KC, Ropelewski C, Wang J, Leetmaa A, Reynolds R, Jenne R, Joseph D (1996) The NCEP/NCAR 40-year reanalysis project. Bull Am Meteorol Soc 77:437–471

Krishnamurty TN, Tewari M, Chakraborty DR, Marengo JA, Silva Dias PL, Satyamurti P (1999) Downstream amplification: a possible precursor to major freeze events over south-eastern Brazil. Weather Forecast 14:242–270

Marengo JA, Cornejo A, Satyamurty P, Nobre C, Sea W (1997) Cold surges in tropical and extratropical South America: the cool event in June 1994. Mon Weather Rev 125:2759–2786

Marengo JA, Ambrizzi T, Kiladis G, Liebmann B (2002) Upper-air wave trains over the Pacific Ocean and wintertime cold surges in

tropical-subtropical South America leading to Freezes in Southern and Southeastern Brazil. Theor Appl Clim 73:223–242

Müller GV (2010) Temperature decrease in the extratropics of South America in response to a tropical forcing during the austral winter. Ann Geophys 28:1–9

Müller GV, Ambrizzi T (2007) Teleconnection patterns and rossby wave propagation associated to generalized frosts over southern South America. Clim Dyn 29(6):633–645

Müller GV, Berri GJ (2007) Atmospheric circulation associated with persistent generalized frosts in central-southern South America. Mon Weather Rev 135(4):1268–1289

Müller GV, Berri GJ (2012) Atmospheric circulation associated with extreme generalized frosts persistence in central-southern South America. Clim Dyn 38(5–6):837–857. doi:10.1007/s00382-011-1113-2

Müller GV, Ambrizzi T, Ferraz SE (2008) The Role of the observed tropical convection in the generation of frost events in the southern cone of South America. Ann Geophys 26:1379–1390

Orlanski I, Katzfey J (1991) The life cycle of a cyclone wave in the Southern Hemisphere. Part I: eddy energy budget. J Atmos Sci 48(17):1972–1998

Orlanski I, Sheldon J (1995) A case of downstream baroclinic development over western North America. Mon Weather Rev 121:2929–2950

Pezza AB, Ambrizzi T (2005) Dynamical conditions and synoptic tracks associated with different types of cold surges over tropical South America. Int J Climatol 25:215–241

Piva ED, Gan MA, Rao VB (2010) Energetics of winter troughs entering South America. Mon Weather Rev 138:1084–1102

Schultz D, Bracken WE, Bosart L, Hakim G, Bedrick M, Dickinson M, Tyle K (1998) Planetary and synoptic-scale signature associated with central American cold surges. Mon Weather Rev 126:5–27

Seluchi ME, Le Treut H, Serafini VY (1998) The impact of the Andes Cordillera on the transient activity: a comparison between observations and the LMS–GCM. Mon Weather Rev 126:895–912

Vera CS, Vigliarolo PK (2000) A Diagnostic Study of Cold-Air Outbreaks over South America. Mon Weather Rev 128:3–24